ANALYSIS-OPERATOR GUIDED SIMULTANEOUS TENSOR DECOMPOSITION AND COMPLETION

Jiaojiao Xiong[1], Sanqian Li[1], Qiegen Liu[1,2,], Xiaoling Xu[1]*

[1] School of Electronic Information Engineering, Nanchang University, Nanchang, 330031, China
[2] Department of Electrical and Computer Engineering, University of Calgary, Calgary, T2N 1N4, Canada

ABSTRACT

Most of low-rank tensor approximation problems are NP-hard. Hence a great number of synthesis tensor decomposition approximation have been proposed. In this paper, we instead present an analysis-operator guided tensor decomposition. The proposed method first employs the classical Field-of-Experts (FoE) filters to produce multi-view features such that forming a higher-order tensor, and then do simultaneous tensor decomposition and completion (STDC). The multi-view features are obtained by convolving the target image with high-frequency FoE filters along different directions and scales. The proposed method is solved efficiently by alternating direction of multipliers method (ADMM). Experiments are conducted to demonstrate the superior performance of our method to state-of-the-art tensor completion methods.

Index Terms—Low-rank tensor, Tensor completion, Field-of-Experts, Multi-view features, ADMM.

1. INTRODUCTION

Low-rank matrix approximation has been successfully applied to real-word problems in recent years, such as inpainting [1-2] and denoising [3]. However, the two-dimensional model cannot fully exploit the correlation in larger data sets such as multispectral data or multidimensional data. As a more general tool to describe the high-dimensional data, low-rank tensor approximation has gained more and more attentions, which is a higher-order extension of low-rank matrix approximation. There are two factorization models: Tucker decomposition [4] and canonical polyadic (CP) decomposition [5].

Despite the difficulty in defining a tensor's rank, a great deal of research efforts have been devoted to understanding low-rank tensor approximation due to a tensor object generally exhibits the structure of the real-world data. Among them low-rank tensor completion is a good example, whose target is to estimate the whole tensor in the case of incomplete observed data [6-9]. Rather than the directly tensor factorization methods are prone to overfitting the model due to an incorrect tensor rank and point estimations of latent factors, subsequently resulting in severe deterioration of predictive performance, completion-based methods exploit an automatic rank optimization, where the rank minimization is formulated as a convex optimization. Liu *et al.* [8] first introduced the trace norm as the convex relaxation of a rank of tensor. In a subsequent work, Liu *et al.* [9] proposed three low-rank tensor completion algorithms to solve the tensor completion of convex optimization. Recently, Wang *et al.* [10] simultaneously imposed the low rank prior and the spatial-temporal consistency for completing videos. To sum up, the above mention methods produce promising results on the visual data with strong global structure. However, they fail on general tensor of visual data. To mitigate the over-strict constraint, [11] used factor priors to simultaneously decompose and complete tensors, which follows the tensor factorization framework proposed in [12] Actually, [11] instead enforced the low rank constraint on the low dimensional representation (submanifold) of the data.

Some researches turn to use the neighbor constraint to improve the performance. Total variation (TV), defined as the l_1-norm of the difference of neighbor elements, is often used to impose piece-wise smoothness constraints. In [13], Ji *et al.* proposed a model combining the total variation regularization and low-rank matrix factorization to recover tensor with missing data. Yang *et al.* [14] extended the TV norm for matrices to higher-order tensors. However, it only takes care of the variations along fibers, and its multi-directionality was limited. To address the problem, Guo *et al.* [15] proposed a generalized tensor TV that considers both the inhomogeneity and the multi-directionality of responses to derivative-like filters definition to exploit the underlying structure of visual data. Yokota *et al.* [16] applied the TV to polyadic decomposition model based tensor completion, and they investigated an additional smoothness constraint that defined as the "l_2-norm" of the difference between neighbor elements. It is worth noting that, although TV-derived techniques has been explored, they still fall into the synthesis representation framework.

The above TV based methods are using only the first derivatives, which can be viewed as the simplest analysis operator. FoE model [17] is higher-order filter-based Markov random field (MRF) model. It contains high-frequency filters as well as derivative filters including the first derivatives along different directions, the second and the third derivatives. These filters enable the higher-order model to capture the structures in images that cannot be captured by using only the first derivatives as in TV based methods. Therefore, we propose to design a FoE filters guided tensor decomposition model, which aims to integrate the strengths of both the conventional synthesis tensor decomposition and analysis operator regularization. In this work, we present a FoE guided simultaneous tensor decomposition and completion (FoE-STDC) method. First, we convolute the target image with FoE filters to formulate multi-view features as tensor. Second, FoE-STDC consisting of the naive STDC model and the STDC based on multi-view features domain are tackled for tensor decomposition and completion.

This work was supported in part by the National Natural Science Foundation of China under 61362001, 6166103, 61503176.

*Correspondence author. E-mail: liuqiegen@ncu.edu.cn.

The remains of this paper are organized as follows. In Section 2, we propose the FoE-STDC model, solved by the augmented Lagrangian (AL) and alternating direction of multipliers method (ADMM). Subsequently, Section 3 demonstrates the performance of the proposed algorithm. Finally, conclusions are given in Section 4.

2. PROPOSED ALGORITHM

2.1. Analysis-operator guided Tensor Completion

Analogous to matrix completion, tensor completion attempts to complete an nth-order tensor $\mathcal{X}_0 \in \mathbb{R}^{I_1 \times I_2 \times \ldots \times I_n}$ from its known entries given by an index set Ω [8, 11, 18-22]. In [8], the nuclear norm of tensor was first applied to tensor completion:

$$\min_{X_{(k)}} \quad \sum_{k=1}^{n} \alpha_k \operatorname{rank}(X_{(k)}) \qquad s.t.\ \ \Omega(\mathcal{X}) = \Omega(\mathcal{X}_0) \tag{1}$$

where $\{\alpha_k\}_{k=1}^{n}$ are defined as weights fulfilling the condition $\sum_{k=1}^{n} \alpha_k = 1$. $X_{(k)}$ denotes the matrix obtained by unfolding tensor $\mathcal{X}$ with respect to mode k. Eq. (1) is approximated by replacing the rank function with nuclear norm $\left\| X_{(k)} \right\|_*$ [8].

More recent sophisticated approaches tried to use the low-rank tensor decomposition for completion, which recover missing data entries while exploiting the factorization structure [11, 16, 19, 20, 21, 22]. To the best of our knowledge, the most state-of-the-art algorithm is the STDC proposed by Chen *et al.* [11]. It incorporates factor priors into simultaneously tensor decomposition and completion as follows:

$$\min_{\hat{\mathcal{X}},\hat{\mathcal{Z}},\hat{\mathbf{V}}_1,\ldots\hat{\mathbf{V}}_n} \sum_{k=1}^{n} \alpha_k \left\| \mathbf{V}_k \right\|_* + \beta \operatorname{tr}\left(\left(\mathbf{V}_1 \otimes \ldots \otimes \mathbf{V}_k \right) \mathbf{L} \left(\mathbf{V}_1 \otimes \ldots \otimes \mathbf{V}_k \right)^{\mathrm{T}} \right) + \gamma \left\| \mathcal{Z} \right\|_{\mathrm{F}}^2$$
$$\text{s.t. } \mathcal{X} = \mathcal{Z} \times_1 \mathbf{V}_1^{\mathrm{T}} \ldots \times_n \mathbf{V}_n^{\mathrm{T}}, \text{ and } \Omega(\mathcal{X}) = \Omega(\mathcal{X}_0) \tag{2}$$

where $\mathcal{Z}$ is the nth-order tensor of the same size as $\mathcal{X}_0$, and each $\mathbf{V}_k$ is an $I_k \times I_k$ matrix. $\times_k$ denotes the mode-k matrix product and $\mathbf{L}$ is the socalled Laplacian matrix. STDC works well to accurately estimate the model factors and missing entries. Nevertheless, like all the existing low-rank tensor approximation, it is still devoted to improve the synthesis decomposition ability.

In this work, we instead consider the analysis sparse representation guided tensor decomposition. Specifically, we investigate the low-rank tensor in the classical FoE filters induced features. FoE filters [17] are the popularly used high-order MRF, which are able to capture the structures in natural images that cannot be captured by only using the first derivatives as in TV filters. The potential function is defined as:

$$p(x,\Theta) = \frac{1}{Z(\Theta)} \prod_{k=1}^{K} \prod_{i=1}^{I} \phi(J_i^T * x_{(k)}; \alpha_i) \tag{3}$$

where $Z(\Theta)$ is the normalizing function; $J_i^T * x_{(k)}$ denotes the convolution of vectorized image $x_{(k)}$ with filter J_i; $\phi(\cdot)$ is an expert function; I stands for the number of experts. The actual FoE model building the filters $\{J_i\}_{i=1}^{I}$ from training dataset BSDS [23] is shown in Fig. 1. Each filter patch can be properly characterized by multiple visual features containing efficient image information such as high-frequency information, edge and texture at various orientations and scales, and multi-view features are complementary to each other.

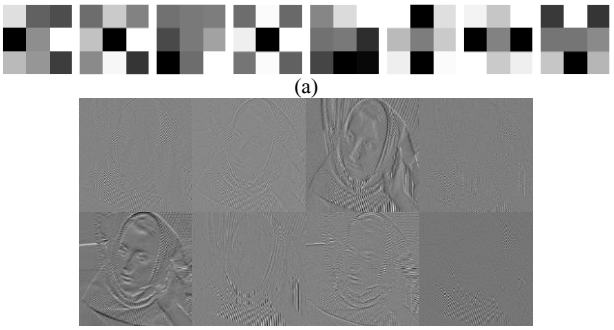

Fig. 1. (a) Learned 3×3 Field-of-Experts filters. (b) Exploration of multi-view features obtained by the convolution of the input image with FoE filters.

Modeling the analysis-operator constrained tensor has two merits. First, the feature-induced tensor has smaller rank values. Considering one color image $\mathcal{X}$ and its one-FoE filter resulting tensor $J_1^T * \mathcal{X}$ as shown in Fig. 2, it can be observed that the associated feature tensor indeed has smaller and more sparse singular values. Second, multi-view features capture high-frequency filters along different directions and scales. This may favor to better represent the high-dimension and high-order information inherent in the original tensor. Furthermore, for any stacked matrix consisting of many component matrices, its rank value is smaller than the rank sum of all the component matrices. i.e., there exists $rank([Y_1, Y_2, \cdots, Y_K]) \le \sum_{k=1}^{K} rank(Y_k)$ [24]. Since the rank of tensor is related to the unfolded matrices at different mode, it motivates us to reformulate all the multi-view features as a whole tensor $[J_1^T, \cdots, J_I^T] * \mathcal{X}$. Therefore, based on the naive STDC, we propose the FoE filter induced STDC as follows:

$$\min_{\hat{\mathcal{X}},\hat{\mathcal{Z}},\hat{\mathbf{V}}_1,\ldots\hat{\mathbf{V}}_n} \sum_{k=1}^{n} \alpha_k \left\| \mathbf{V}_k \right\|_* + \beta \operatorname{tr}\left(\left(\mathbf{V}_1 \otimes \ldots \otimes \mathbf{V}_n \right) \mathbf{L} \left(\mathbf{V}_1 \otimes \ldots \otimes \mathbf{V}_n \right)^{\mathrm{T}} \right) + \gamma \left\| \mathcal{Z} \right\|_{\mathrm{F}}^2$$
$$\text{s.t. } [\mathrm{J}_1^{\mathrm{T}}, \cdots, \mathrm{J}_{\mathrm{I}}^{\mathrm{T}}] * \mathcal{X} = \mathcal{Z} \times_1 \mathbf{V}_1^{\mathrm{T}} \ldots \times_n \mathbf{V}_n^{\mathrm{T}} \text{ and } \Omega(\mathcal{X}) = \Omega(\mathcal{X}_0) \tag{4}$$

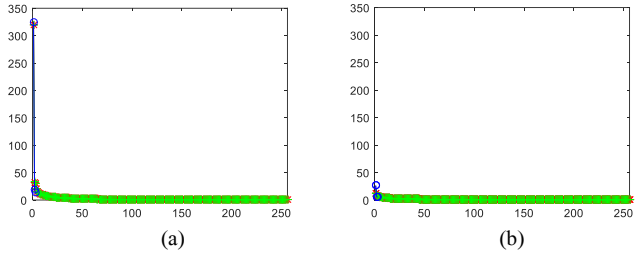

(a) (b)

Fig. 2. Singular values of three unfolding matrices of the original tensor (a) and the associated feature tensor (b).

2.2. Proposed FoE-STDC

According to the above analysis, we propose a novel algorithm called FoE-STDC, combining the naive STDC and high-order

STDC based on analysis-operator derived features, is as follows:

$$\min_{\mathcal{X},\hat{\mathcal{Z}}_1,\hat{\mathcal{Z}}_2,\hat{\mathbf{V}}_1^1\ldots\hat{\mathbf{V}}_n^1,\hat{\mathbf{V}}_1^2\ldots\hat{\mathbf{V}}_n^2} \beta_1 \operatorname{tr}\left(\left(\mathbf{V}_1^1\otimes\ldots\otimes\mathbf{V}_k^1\right)\mathbf{L}\left(\mathbf{V}_1^1\otimes\ldots\otimes\mathbf{V}_k^1\right)^{\mathrm{T}}\right)+\sum_{k=1}^{n}\alpha_k^1\left\|\mathbf{V}_k^1\right\|_*+\gamma_1\left\|\mathcal{Z}_1\right\|_{\mathrm{F}}^2$$
$$+\eta\left(\sum_{k=1}^{n}\alpha_k^2\left\|\mathbf{V}_k^2\right\|+\gamma_2\left\|\mathcal{Z}_2\right\|_{\mathrm{F}*}^2+\beta_2\operatorname{tr}\left(\left(\mathbf{V}_1^2\otimes\ldots\otimes\mathbf{V}_k^2\right)\mathbf{L}\left(\mathbf{V}_1^2\otimes\ldots\otimes\mathbf{V}_k^2\right)^{\mathrm{T}}\right)\right)$$
$$\text{s.t. } \mathcal{X}=\mathcal{Z}_1\times_1\mathbf{V}_1^{1\mathrm{T}}\ldots\times_n\mathbf{V}_n^{1\mathrm{T}},\ [\mathrm{J}_1^{\mathrm{T}},\cdots,\mathrm{J}_I^{\mathrm{T}}]*\mathcal{X}=\mathcal{Z}_2\times_1\mathbf{V}_1^{2\mathrm{T}}\ldots\times_n\mathbf{V}_n^{2\mathrm{T}}$$
$$\text{and } \Omega(\mathcal{X})=\Omega(\mathcal{X}_0) \tag{5}$$

where η is the weight of feature domain in the model. To solve (5) with a large number of unknowns and equality constraints, by introducing additional variables $\mathcal{B}=[J_1^T,\cdots,J_I^T]*\mathcal{X}$, the AL is used to convert it into unconstraint minimization problem as follows:

$$\min_{\mathcal{X},\hat{\mathcal{Z}}_1,\hat{\mathcal{Z}}_2,\mathbf{V}_1^1\ldots\mathbf{V}_n^1,\mathbf{V}_1^2\ldots\mathbf{V}_n^2,\mathcal{Y}_1,\mathcal{Y}_1,\mathcal{B},\mathcal{W}} \beta_1 tr\left(\left(\mathbf{V}_k^1\otimes\ldots\otimes\mathbf{V}_k^1\right)\mathbf{L}\left(\mathbf{V}_k^1\otimes\ldots\otimes\mathbf{V}_k^1\right)^{T}\right)$$
$$+\sum_{k=1}^{n}\alpha_k^1\left\|\mathbf{V}_k^1\right\|+\gamma_1\left\|\mathcal{Z}_1\right\|_F^2+\frac{\mu_1}{2}\left\|\frac{\mathcal{Y}_1}{\mu_1}+\mathcal{X}-\mathcal{Z}_1\times_1\mathbf{V}_1^{1\mathrm{T}}\ldots\times_n\mathbf{V}_n^{1\mathrm{T}}\right\|_{\mathrm{F}}^2$$
$$+\eta\left(\sum_{k=1}^{n}\alpha_k^2\left\|\mathbf{V}_k^2\right\|_*+\beta_2 tr\left(\left(\mathbf{V}_k^2\otimes\ldots\otimes\mathbf{V}_k^2\right)\mathbf{L}\left(\mathbf{V}_k^2\otimes\ldots\otimes\mathbf{V}_k^2\right)^{T}\right)+\gamma_2\left\|\mathcal{Z}_2\right\|_F^2\right.$$
$$\left.+\frac{\mu_2}{2}\left\|\frac{\mathcal{Y}_2}{\mu_2}+\mathcal{B}-\mathcal{Z}_2\times_1\mathbf{V}_1^{2\mathrm{T}}\ldots\times_n\mathbf{V}_n^{2\mathrm{T}}\right\|_{\mathrm{F}}^2+\frac{\lambda}{2}\left\|\frac{\mathcal{W}}{\lambda}+\mathcal{B}-[\mathrm{J}_1^{\mathrm{T}},\cdots,\mathrm{J}_I^{\mathrm{T}}]*\mathcal{X}\right\|_{\mathrm{F}}^2\right) \tag{6}$$

The ADMM [25, 26], via alternating minimization with respect to one variable while keeping other variables fixed, can be used to address the minimization of Eq. (6) with respect to $\mathbf{V}_1^1,\ldots\mathbf{V}_n^1,\mathbf{V}_1^2,\ldots\mathbf{V}_n^2,\mathcal{Z}_1,\mathcal{Z}_2,$ $\mathcal{B}$ and $\mathcal{X}$.

Updating the $\mathbf{V}_k^1$ and $\mathbf{V}_k^2$

$$\hat{\mathbf{V}}_k^1=\arg\min_{\mathbf{V}_k^1}\left\|\mathbf{V}_k^1\right\|_*+\beta_1\operatorname{tr}\left(\mathbf{V}_k^1\mathbf{H}_k^{1,T}\mathbf{H}_k^1\mathbf{V}_k^{1,T}\right)+\frac{\mu_1}{2}\left\|\frac{\mathbf{Y}_1^{(k)}}{\mu}+\mathbf{X}^k-\mathbf{V}_k^{1,T}\mathbf{Z}_1^{(k)}\mathbf{U}_k^1\right\|_F^2$$
$$\textit{and }\ \mathbf{U}_k^1=\mathbf{V}_1^1\otimes\ldots\otimes\mathbf{V}_{k-1}^1\otimes\mathbf{V}_{k+1}^1\otimes\ldots\otimes\mathbf{V}_n^1 \tag{7}$$

$$\hat{\mathbf{V}}_k^2=\operatorname*{argmin}_{\mathbf{V}_k^1}\alpha_k^2\left\|\mathbf{V}_k^2\right\|_*+\beta_2 tr\left(\mathbf{V}_k^2\mathbf{H}_k^{2,T}\mathbf{H}_k^2\mathbf{V}_k^{2,T}\right)$$
$$+\frac{\mu_2}{2}\left\|\frac{\mathbf{Y}_2^{(k)}}{\mu}+\mathbf{B}^k-\mathbf{V}_k^{2,T}\mathbf{Z}_2^{(k)}\mathbf{U}_k^2\right\|_{\mathrm{F}}^2 \tag{8}$$

We use the same technique in STDC to solve (7) and (8).

Updating the $\mathcal{Z}_1$ and $\mathcal{Z}_2$

$$\hat{\mathcal{Z}}_1=\operatorname*{argmin}_{\hat{\mathcal{Z}}_2}\gamma_1\left\|\mathcal{Z}_1\right\|_{\mathrm{F}}^2+\frac{\mu_1}{2}\left\|\left(\mathcal{X}+\frac{\mathcal{Y}_1}{\mu_1}\right)-\mathcal{Z}_1\times_1\mathbf{V}_1^{1\mathrm{T}}\ldots\times_n\mathbf{V}_n^{1\mathrm{T}}\right\|_{\mathrm{F}}^2 \tag{9}$$

By using conjugate gradient (CG) descent as in [11], the solver is obtained. Similarly, the solver of Eq. (10) is same as the Eq. (9).

$$\hat{\mathcal{Z}}_2=\operatorname*{argmin}_{\hat{\mathcal{Z}}_2}\gamma_2\left\|\mathcal{Z}_2\right\|_{\mathrm{F}}^2+\frac{\mu_2}{2}\left\|\left(\mathcal{B}+\frac{\mathcal{Y}_2}{\mu_2}\right)-\mathcal{Z}_2\times_1\mathbf{V}_1^{2\mathrm{T}}\ldots\times_n\mathbf{V}_n^{2\mathrm{T}}\right\|_{\mathrm{F}}^2 \tag{10}$$

Updating the $\mathcal{B}$

$$\mathcal{B}=\operatorname*{argmin}_{\mathcal{B}}\frac{\mu_2}{2}\left\|\frac{\mathcal{Y}_2}{\mu_2}+\mathcal{B}-\mathcal{Z}_2\times_1\mathbf{V}_1^{2\mathrm{T}}\ldots\times_n\mathbf{V}_n^{2\mathrm{T}}\right\|_{\mathrm{F}}^2+\frac{\eta\lambda}{2}\left\|\frac{\mathcal{W}}{\lambda}+\mathcal{B}-[\mathrm{J}_1^{\mathrm{T}},\cdots,\mathrm{J}_I^{\mathrm{T}}]*\mathcal{X}\right\|_{\mathrm{F}}^2 \tag{11}$$

The least squares solution satisfies the normal equation.

Updating the $\mathcal{X}$

$$\mathcal{X}=\operatorname*{argmin}_{\mathcal{X}}\frac{\mu_1}{2}\left\|\frac{\mathcal{Y}_1}{\mu_1}+\mathcal{X}-\mathcal{Z}_1\times_1\mathbf{V}_1^{1\mathrm{T}}\ldots\times_n\mathbf{V}_n^{1\mathrm{T}}\right\|_{\mathrm{F}}^2+\frac{\eta\lambda}{2}\left\|\frac{\mathcal{W}}{\lambda}+\mathcal{B}-[\mathrm{J}_1^{\mathrm{T}},\cdots,\mathrm{J}_I^{\mathrm{T}}]*\mathcal{X}\right\|_{\mathrm{F}}^2 \tag{12}$$

The entire FoE-STDC algorithm is summarized as follows:

Algorithm 1: FoE-STDC

Input: an incomplete tensor $\mathcal{X}_0\in\mathbb{R}^{I_1\times I_2\times\ldots\times I_n}$, matrix $\mathbf{L}$.

1: Initialize $\mathcal{X},\mathbf{V}_1^1,\ldots\mathbf{V}_n^1,\mathbf{V}_1^2,\ldots\mathbf{V}_n^2,\mathcal{Z}_1,\mathcal{Z}_2,\mathcal{Y}_1,\mathcal{Y}_2,\mathcal{B},\mathcal{W}$ by $\mathbf{V}_k=\mathrm{I}\ (1\le k\le n)$, $\mathcal{Z}=\mathcal{X}=\mathcal{X}_0$ and $\mathcal{Y}=0$

2: **For** $t=1,2,\cdots$ repeat until a stop-criterion is satisfied

3: update $\mathbf{V}_k^1$ and $\mathbf{V}_k^2$ via Eq. (7) and (8)

4: update $\mathcal{Z}_1$ and $\mathcal{Z}_2$ via Eq. (9) and (10)

5: update $\mathcal{B}$ via Eq. (11)

6: update $\mathcal{X}$ via Eq. (12)

7: update $\mathcal{Y}_1$ via $\mathcal{Y}_1^{t+1}=\mathcal{Y}_1^t+\mu_1^t\left(\mathcal{X}-\mathcal{Z}\times_1\mathbf{V}_1^{1\mathrm{T}}\ldots\times_n\mathbf{V}_n^{1\mathrm{T}}\right)$ and $\mathcal{Y}_2$ via $\mathcal{Y}_2^{t+1}=\mathcal{Y}_2^t+\mu_2^t\left(\mathcal{B}-\mathcal{Z}\times_1\mathbf{V}_1^{2\mathrm{T}}\ldots\times_n\mathbf{V}_n^{2\mathrm{T}}\right)$

8: update $\mathcal{W}$ via $\mathcal{W}_1^{t+1}=\mathcal{W}_1^t+\lambda^t\left(\mathcal{B}-[\mathrm{J}_1^{\mathrm{T}},\cdots,\mathrm{J}_I^{\mathrm{T}}]*\mathcal{X}\right)$

9: $\mu_1^{t+1}=\rho\mu_1^t,\mu_2^{t+1}=\rho\mu_2^t,\rho\in[1.1,1.2]$

10: **End**

Output: $\mathcal{X},\mathbf{V}_1^1,\ldots\mathbf{V}_n^1,\mathbf{V}_1^2,\ldots\mathbf{V}_n^2,\mathcal{Z}_1,\mathcal{Z}_2$ and $\mathcal{B}$

3. EXPERIMENTAL RESULTS

In this section, the performance of proposed algorithm is evaluated for image inpainting, and compare with the state-of-the-art methods: M^{2}SA [27], M^{2}SA-G [12], HaLRTC [9] and STDC. We use the RSE and PSNR to evaluate the recovery quality. In all the experiments, we use a fixed FoE filter set in refs. [17, 28] denoted by csf_3×3 to construct 8 different multi-view features. The proposed method mainly involves two parameters λ and η. For better recovery performance, the two parameters need to be tuned separately for each missing ratio and different image. Generally, the value of λ and η are in the range of $[10^{-2}, 2\times10^{-2}]$ and $[0.1, 1.5]$, respectively.

Experiments are conducted on eight benchmark images shown in Fig. 3. We generate incomplete data by deleting elements of the images randomly, with different missing ratios $\in\{70, 80, 90\}$. The corresponding PSNR and RSE results by different methods are listed in Table 1. Overall, the proposed method exhibits more accurate recovery with larger PSNR and lower RSE values than M^{2}SA, M^{2}SA-G, HaLRTC and STDC methods. Particularly in the case of 70%, the average PSNR of FoE-STDC outperforms STDC with marked improvement 1.16

dB. To facilitate the evaluation subjective comparison, the recovery results by the four competing methods for image with 90% missing ratio are compared in Fig 4. It can be seen that STDC achieves better recovery performance than M^{2}SA, M^{2}SA-G and HaLRTC. However, it produces over-smoothed results and eliminates many image details. The FoE-STDC in the last column outperforms STDC method. Particularly, it well preserves the image edges and texture and recovers the missing information more effectively (see the enlargement).

Fig. 3. The photographic images for test. *Airplane, Baboon, Barbara, Façade, Barbara, Lena, Peppers, and Sailboat.* $256\times256\times3$.

4. CONCLUSIONS

This paper presents a FoE guided simultaneous tensor decomposition and completion model, which tends to explore the low-rank priority on the analysis representation-induced tensor. It inherits the strengths of analysis representation with characteristic of multi-view sparse features and STDC with synthesis decomposition. Efficient ADMM technique is employed to tackle the resulting optimization. Experiment results has illustrate the clear advantages of our method over state-of-the-art algorithms, such as HaLRTC and STDC methods.

Table 1: The averaged recovery performance (PSNR/RSE) on eight images with missing rates of 70%, 80% and 90%

	Method	*Airplane*	*Baboon*	*Barbara*	*Facade*	*House*	*Lena*	*Peppers*	*Sailboat*	*Average*
70%	M^{2}SA	23.77/.1081	21.18/.1921	24.35/.1316	27.66/.1028	26.12/.1051	23.60/.1302	23.72/.1386	21.90/.1718	24.04/.1375
	M^{2}SA-G	26.28/.0837	22.11/.1787	26.49/.1115	28.22/.0989	28.40/.0875	26.56/.1113	26.20/.1243	24.08/.1446	26.04/.1176
	HaLRTC	25.22/.0928	22.61/.1719	26.30/.1132	29.18/.0927	28.53/.0967	26.25/.1139	25.15/.1339	23.64/.1493	25.86/.1193
	STDC	27.64/.0625	23.03/.1428	28.19/.0864	29.54/.0667	30.72/.0527	28.86/.0731	27.78/.0828	27.90/.1061	27.96/.0841
	FoE-STDC	**29.07/.0554**	**23.71/.1306**	**28.58/.0832**	**31.12/.0568**	**31.26/.0496**	**30.03/.0626**	**31.20/.0786**	**27.97/.1053**	**29.12/.0741**
80%	M^{2}SA	21.04/.1438	19.63/.1687	21.16/.1417	25.55/.0854	22.17/.1260	20.75/.1483	20.60/.1511	19.78/.1659	21.34/.1414
	M^{2}SA-G	24.11/.1211	21.38/.1581	25.08/.1101	26.87/.0934	26.59/.0958	25.24/.1186	24.93/.1118	22.55/.1307	24.59/.1174
	HaLRTC	22.86/.1366	21.23/.1706	23.64/.1365	27.56/.1078	25.66/.1244	23.73/.1252	22.40/.1230	21.46/.1370	23.57/.1301
	STDC	26.50/.0731	21.84/.1720	26.73/.1015	28.32/.0812	30.01/.0613	28.00/.0838	27.42/.0956	25.02/.1246	26.73/.0991
	FoE-STDC	**27.77/.0717**	**22.85/.1449**	**27.59/.0968**	**28.53/.0790**	**30.26/.0598**	**28.22/.0791**	**27.51/.0901**	**25.25/.1173**	**27.25/.0923**
90%	M^{2}SA	16.72/.2505	17.41/.2314	15.81/.2781	21.77/.1399	17.47/.2296	15.96/.2729	15.91/.2748	16.29/.2628	17.17/.2425
	M^{2}SA-G	21.14/0.150	20.38/.1642	22.31/.1314	23.42/.1157	23.21/.1186	22.45/.1295	22.03/.1359	20.27/.1667	21.90/.1391
	HaLRTC	20.10/.1697	19.27/.1867	20.00/.1716	25.51/.0910	22.01/.1361	20.45/.1630	18.27/.2095	18.68/.1997	20.54/.1659
	STDC	**24.45**/.0977	20.60/.2047	24.19/.1391	25.07/.1199	26.97/.0889	25.48/.1090	24.29/.1291	22.40/.1607	24.18/.1311
	FoE-STDC	24.40/**.0907**	**21.29/.1747**	**24.82/.1267**	**25.48/.1129**	**27.52/.0834**	**26.47/.0952**	**24.54/.1181**	**22.48/.1493**	**24.63/.1189**

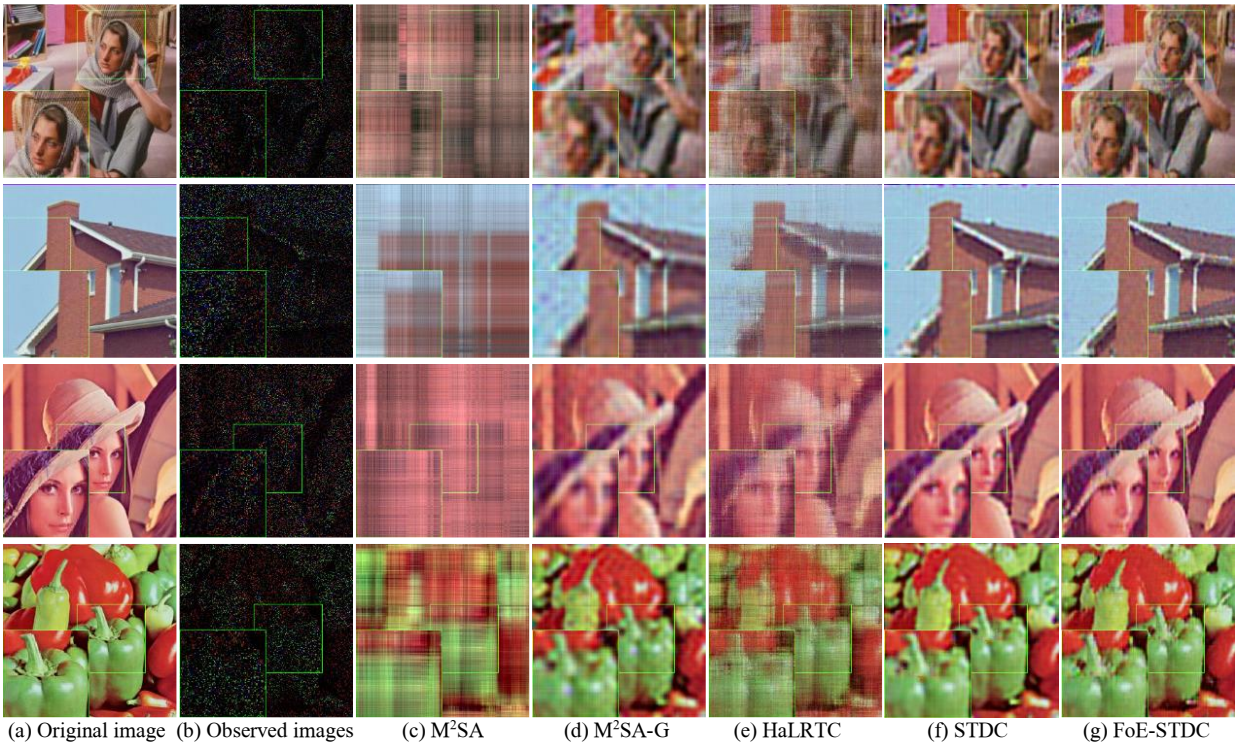

(a) Original image (b) Observed images (c) M^{2}SA (d) M^{2}SA-G (e) HaLRTC (f) STDC (g) FoE-STDC

Fig.4. Recover images with 90% of missing using different methods M^{2}SA, M^{2}SA-G, HaLRTC, STDC, FoE-STDC.

5. REFERENCES

[1] T. Ding, M. Sznaier, and O.I. Camps, "A rank minimization approach to video inpainting," *Proc. 11th IEEE Int'l Conf. Computer Vision (ICCV)*, pp. 1-8, 2007.

[2] Y. Wang and Y. Zhang, "Image inpainting via weighted sparse non-negative matrix factorization," *Proc. 18th IEEE Int'l Conf. Image Processing (ICIP)*, pp. 3409-3412, 2011.

[3] H. Ji, C. Liu, Z. Shen, and Y. Xu, "Robust video denoising using low rank matrix completion," *Proc. IEEE Conf. Computer Vision and Pattern Recognition (CVPR)*, pp. 1791-1798, 2010.

[4] L. R. Tucker, "Implications of factor analysis of three-way matrices for measurement of change," *In Problems in Measuring Change*, pp. 122-137. University of Wisconsin Press, 1963.

[5] H. A. Kiers, "Towards a standardized notation and terminology in multiway analysis," *Journal of Chemometrics*, vol. 14, no. 3, pp. 105-122, 2000.

[6] E. Acar, D.M. Dunlavy, T.G. Kolda, and M. Morup, "Scalable tensor factorization for incomplete data," *Chemometrics and Intelligent Laboratory Systems*, vol. 106, pp. 41-56, 2011.

[7] X. Geng, K. Smith-Miles, Z.H. Zhou, and L. Wang, "Face image modeling by multilinear subspace analysis with missing values," *IEEE Trans. Systems, Man, and Cybernetics—Part B: Cybernetics*, vol. 41, no. 3, pp. 881-892, June 2011.

[8] J. Liu, P. Wonka, and J. Ye, "Tensor completion for estimating missing values in visual data," *Proc. 12th IEEE Int'l Conf. Computer Vision (ICCV)*, 2009.

[9] J. Liu, P. Musialski, P. Wonka, and J. Ye, "Tensor completion for estimating missing values in visual data," *IEEE Trans. Pattern Analysis and Machine Intelligence,* vol. 35, no.1, pp. 208-220, Jan. 2013.

[10] H. Wang, F. Nie, and H. Huang, "Low-rank tensor completion with spatio-temporal consistency," *In Proceedings of AAAI Conference on Artificial Intelligence (AAAI)*, pp. 2846–2852, 2014.

[11] Y. L. Chen, C. T. Hsu, and H. Y. M. Liao, "Simultaneous tensor decomposition and completion using factor priors," *IEEE Trans. Pattern Analysis and Machine Intelligence,* vol. 36, no. 3, pp. 577-591, 2014.

[12] A. Narita, K. Hayashi, R. Tomioka, and H. Kashima, "Tensor factorization using auxiliary information," *In Proceedings of Machine Learning and Knowlegde Discovery in Databases*, pp. 501-516, 2011.

[13] T. Ji, T. Huang, X. Zhao, T. Ma, G. Liu, "Tensor completion using total variation and low-rank matrix factorization," *Information Sciences,* 326: pp. 243–257, 2016.

[14] S. Yang, J. Wang, W. Fan, X. Zhang, P. Wonka, and J. Ye, "An efficient admm algorithm for multimensional anisotropic toal variation regularization problems," I*n Proceedings of ACM SIGKDD International Conference on Knowledge Discovery and Data Mining (KDD)*, pp. 641-649, 2013.

[15] X. Guo, and Y. Ma. "Generalized tensor total variation minimization for visual data recovery?," *in (CVPR), IEEE Conference on,* pp. 3603-3611, 2015.

[16] T. Yokota, Q. Zhao, and A. Cichocki, "Smooth parafac decomposition for tensor completion," *arXiv:1505.06611*, 2016. [Online].

[17] S. Roth, and M. J. Black, "Fields of Experts," International Journal of Computer Vision, vol. 82, no. 2, pp. 205-229, 2009.

[18] S. Gandy, B. Recht, and I. Yamada, "Tensor completion and low-n-rank tensor recovery via convex optimization," *Inv. Probl., vol. 27*, no. 2, pp.025010, Jan 2011.

[19] H. Tan, B. Cheng, W. Wang, Y.-J. Zhang, and B. Ran, "Tensor completion via a multi-linear low-n-rank factorization model," *Neurocomputing,* vol. 133, pp. 161–169, Jun 2014.

[20] P. Rai, Y. Wang, S. Guo, G. Chen, D. Dunson, and L. Carin, "Scalable Bayesian low-rank decomposition of incomplete multiway tensors," *In Proceedings of the 31st International Conference on Machine Learning (ICML-14)*, pp. 1800–1808, 2014.

[21] L. Sorber, M. Van Barel, and L. De Lathauwer, "Optimization-based algorithms for tensor decompositions: Canonical polyadic decomposition, decomposition in rank-(Lr, Lr, 1) terms, and a new generalization," *SIAM Journal on Optimization*, 23(2):695–720, 2013.

[22] Q. Zhao, L. Zhang, and A. Cichocki, "Bayesian CP factorization of incomplete tensors with automatic rank determination," *IEEE Transactions on Pattern Analysis and Machine Intelligence*, 37(9):1751–1763, 2015.

[23] D. Martin, C. Fowlkes, D. Tal, J. Malik, "A database of human segmented natural images and its application to evaluating segmentation algorithms and measuring ecological statistics," *in: IEEE International Conference on Computer Vision (ICCV), IEEE,* pp. 416–423, 2001.

[24] Q. Qiu, and G. Sapiro, "Learning transformations for clustering and classification," *Journal of Machine Learning Research,* vol. 16, pp. 187-225, 2015.

[25] M. Afonso, J. Bioucas-Dias, and M. Figueiredo, "An augmented lagrangian approach to the constrained optimization formulation of imaging inverse problems," *IEEE Trans. Image Process.*, vol. 20, no. 3, pp. 681–695, 2011.

[26] Q. Liu, D. Liang, Y. Song, J. Luo, Y. Zhu, W. Li, "Augmented Lagrangian based sparse representation method with dictionary updating for image deblurring," *SIAM Journal on Imaging Science*, vol. 6, no. 3, pp. 1689-1718, 2013.

[27] X. Geng, K. Smith-Miles, Z.H. Zhou, and L. Wang, "Face image modeling by multilinear subspace analysis with missing values," *IEEE Trans. Systems, Man, and Cybernetics-Part B: Cybernetics*, vol. 41, no. 3, pp. 881-892, June 2011

[28] U. Schmidt and S. Roth, "Shrinkage fields for effective image restoration," *in (CVPR), IEEE Conference on,* pp. 2774-2781. 2014.